

# Dusty Casson's Oscillatory Flow Between Parallel Plates

<sup>[1]</sup> Rafiuddin, <sup>[2]</sup> S.A. Hussaini

<sup>[1]</sup> Humanities and Science Department, CVR College of Engineering, Ibrahimpatnam, RR Dist., Telangana, India.

<sup>[2]</sup> Humanities and Science Department, Muffakham Jah College of Engineering & Technology, Banjara Hills, Hyderabad, Telangana, India.

---

**Abstract:--** A numerical solution is obtained for the unsteady dusty flow between two parallel plates. The flow is investigated for two cases. In case-1, the lower plate is executing simple harmonic oscillations in its own plane and upper plate is fixed and in case-2, both the plates are vibrating with same amplitude and frequency. Expressions for velocity profiles and skin friction are found for the above cases. Graphs are shown and the results are discussed taking into account the effect of Casson and other parameters.

---

## 1. INTRODUCTION

NPs flow has become a subject of an immense interest because of its diverse applications. NPs have large surface area and nano scale size, their properties depend on size, shape and structures and has commercial usage (in manufacture of scratch proof glasses, self clearing windows, crack resistant paints, anti graffiti coatings for wall, transparent sunscreen, stain repellent fabrics), medical applications (anti microbial application, bio sensing, imaging, drug delivery, hyperthermic treatment for malignant cells), environment applications (bio remediation of diverse contaminants, water treatment and production of clean energy) and has applications in food science and industrial production. Mujumdar and Minco (2019) investigated the nano carrier based systems for targeted and specific therapeutic delivery. Hussain *et al.* (2019) examined dusty casson nano fluid with thermal radiation and found that heat of nano fluid increases with radiation parameter. Hussain *et al.* (2018) studied the time dependent MHD radiative flow and heat transfer of dusty casson nano fluid and concluded that radiation parameter rise the temperature profile of dusty nano fluid. Narender *et al.* (2018) highlighted the radiation effect on magnetic stagnation point flow of nano fluid and deduced that heat transfer enhances with radiation parameter.

Fluid flow under the influence of magnetic field and heat transfer takes place in magneto-hydrodynamics, accelerators, pumps and generators. Abbas *et al.* (2019) found slip effects on magnetic dusty flow by analytical perturbation method as well as numerical tool of Runge-Kutta method of order four, the outcomes are in total agreement. Ali *et al.* (2019) considered the flow of dust particles and memory fluid, found that the velocities of dust and fluid phase using finite difference method and concluded that viscosity ratio is

accountable for higher velocity of dust phase. Ismail *et al.* (2018) obtained the solution of unsteady magnetic dusty flow between the parallel plates and ascertained that dust particles have higher velocity than fluid. Sasikala *et al.* (2018) analyzed the Stokes dusty flow in porous medium and shown that magnetic parameter suppresses the velocity profiles of fluid and dust particles. Selvi and Srinivas (2018) examined the oscillatory flow of a Casson fluid in an elastic tube with variable cross-section. Jalil *et al.* (2017) obtained the exact solution of boundary layer dusty flow using suitable similarity transformations. Kumar and Srinivas (2017) studied the simultaneous effects of thermal radiation and chemical reaction on hydrodynamic pulsatile flow of a Casson fluid in porous space. Imran *et al.* (2016) presented the effects of slip on free convection flow of Casson fluid over an oscillating porous plate and found that slip subsided the velocity field. Khalid *et al.* (2015) discussed the time dependent magnetic convective Casson flow past oscillating vertical plate in porous medium and exact solution is obtained for velocity and energy field using Laplace technique. Pramanik (2014) highlighted Casson fluid flow and heat transfer past an exponentially porous stretching surface in presence of thermal radiation.

Dusty fluid flow has applications like waste water treatment, power plant piping, combustion, petroleum transport and flow meters. Singh *et al.* (2017) discussed unsteady free convective oscillatory flow of variable permeability and depicted that permeability parameter mitigates the mean velocity profiles. Vidhya *et al.* (2017) presented free convective and oscillatory flow of dusty fluid through porous medium and demonstrated that dust particles influence the velocity of fluid compared to clean fluid profiles. Prasuna and Sushma (2015) explored the second order fluid flow in

porous media between two oscillating parallel plates and concluded that the coefficient of porosity is to diminish velocity profiles up to the middle of channel, thereafter velocity shoots up. Now aim is to study dusty oscillatory memory flow between parallel plates, whose constitutive equation is given by Casson.

The rheological equation of state for an isotropic and incompressible Casson fluid flow (1959) is

$$\begin{aligned} \tau_{ij} &= 2 \left( \mu_B + \frac{p_y}{\sqrt{2\pi}} \right) e_{ij}, \pi > \pi_c \\ &= 2 \left( \mu_B + \frac{p_y}{\sqrt{2\pi c}} \right) e_{ij}, \pi < \pi_c \end{aligned}$$

Here,  $\tau_{ij}$  is the (i,j)-th component of the stress tensor,  $\pi = e_{ij}e_{ij}$  and  $e_{ij}$  are the (i,j)-th component of the deformation rate,  $\pi$  is the product of the component of deformation rate with itself,  $\pi_c$  is a critical value of this product based on the non-Newtonian model,  $\mu_B$  is plastic dynamic viscosity of the non-Newtonian fluid, and  $p_y$  is the yield stress of the fluid. So, if a shear stress less than the yield stress are applied to the fluid, it behaves like a solid, whereas if a shear stress greater than yield stress is applied, it starts to move.

Let the fluid motion be along the lower plate, that is x-axis direction and y-axis is orthogonal to it. Let u,v,w be the velocity components for the study, take v=0 and w=0 and the variations in u are with respect to y and t is only considered.

An instant velocity for the present study is  $u = \text{Re} (u_0 e^{-i\omega t})$ , where 'Re' signifies real part and we omit 'Re' and take real part of the final outcome.

**Case-1:** Upper plate is fixed and lower plate is performing simple harmonic oscillations in its own plane. Here velocity u is a function of y and t, the equation of momentum in absence of body forces is

$$\begin{aligned} &\frac{\partial u}{\partial t} \\ &= \vartheta \left( 1 + \frac{1}{\alpha} \right) \frac{\partial^2 u}{\partial y^2} - \frac{\vartheta u}{k} \\ &+ \frac{KN(v_p - u)}{\rho} \end{aligned} \quad (1)$$

$$= \frac{K}{m} (u - v_p) \quad (2)$$

$$= 0 \quad (3)$$

Boundary conditions are

$$u(0, t) = u_0 e^{-i\omega t}, \quad u(2y_0, t) = 0 \quad (4)$$

Introducing dimensionless quantities

$$\begin{aligned} \bar{u} &= \frac{u}{u_0}, \quad \bar{y} = \frac{y}{y_0}, \quad \bar{t} = \frac{t\vartheta}{y_0^2}, \quad \bar{k} = \frac{k}{y_0^2}, \\ \bar{v}_p &= \frac{y_0 v_p}{\vartheta}, \quad \tau = \frac{m\vartheta}{Ky_0^2}, \quad \bar{\omega} = \frac{\omega y_0^2}{\vartheta} \end{aligned} \quad (5)$$

Using (5) into (1) and (2), we get

$$\frac{\partial \bar{u}}{\partial \bar{t}} = \left( 1 + \frac{1}{\alpha} \right) \frac{\partial^2 \bar{u}}{\partial \bar{y}^2} - \left( \frac{l}{\tau} + \frac{1}{k} \right) \bar{u} + \frac{l v_p}{\tau} \quad (6)$$

$$\tau \frac{\partial v_p}{\partial t} = (u - v_p) \quad (7)$$

Eliminating  $v_p$  from equation (6) using equation (7), we get

$$\begin{aligned} \frac{\partial^2 \bar{u}}{\partial \bar{t}^2} &= \left( 1 + \frac{1}{\alpha} \right) \frac{\partial^3 \bar{u}}{\partial \bar{t} \partial \bar{y}^2} + \frac{1}{\tau} \left( 1 + \frac{1}{\alpha} \right) \frac{\partial^2 \bar{u}}{\partial \bar{y}^2} - \left( \frac{l+1}{\tau} + \frac{1}{k} \right) \frac{\partial \bar{u}}{\partial \bar{t}} \\ &\quad - \frac{\bar{u}}{\tau k} \end{aligned} \quad (8)$$

Where

K – stock's coefficient of resistance ( $6\pi\mu$ ) for spherical dust particles

a – average radius of dust particle

$\mu$  – viscosity of the fluid

u- velocity of fluid

$v_p$ - velocity of dust particle

l –  $mN / \rho$  mass concentration of dust particle

$\rho$  – density of fluid

m – average mass of dust particle

N – number of dust particle per unit volume

$\tau$  – m/K relaxation time

$\omega$  - frequency parameter

$\vartheta$  – kinematic viscosity

k – permeability parameter

$y_0$  – characteristic length

$\alpha$  - Casson's parameter and

$2y_0$ - the clearance distance between the plates

The dimensionless boundary conditions are

$$u(0, t) = e^{-i\omega t}, \quad u(2, t) = 0 \quad (9)$$

Let

$$u = f(y) e^{-i\omega t} \quad (10)$$

be the supposed solution of (8), then equation (6) give rise to

$$f''(y) + mf(y) = 0 \quad (11)$$

Using (9) and (10), we get

$$f(0) = 1 \text{ and } f(2) = 0 \quad (12)$$

Where

$i b_2)$

The numerical solution of ordinary differential equation (11) subject to boundary conditions (12) using Galerkin technique of finite element analysis is

$$m = \frac{\alpha}{1+\alpha} (a_2 + i b_2) \quad (13)$$

$$f(y) = \frac{1}{2}(2-y) + (A+iB)(y^2-2y) \quad (14)$$

The equations (14) and (10) give rise to real part of fluid velocity profile as

$$u_1(y) = \frac{1}{2}(2-y) \cos \omega t + (y^2-2y)(A \cos \omega t + B \sin \omega t) \quad (15)$$

Skin friction of fluid is

$$Sf_1 = \left( \frac{\partial u_1}{\partial y} \right)_{y=0} = -\frac{1}{2} \cos \omega t - 2(A \cos \omega t + B \sin \omega t) \quad (16)$$

Equation (6) yields dust velocity

$$v_{p1} = \frac{\tau}{l} \left[ \left\{ B \left( \frac{l}{\tau} + \frac{1}{k} \right) (y^2-2y) - 2B - A\omega(y^2-2y) - \frac{\omega}{2}(2-y) \right\} \sin \omega t + \left\{ B\omega(y^2-2y) - 2A + \left( \frac{l}{\tau} + \frac{1}{k} \right) \left\{ A(y^2-2y) + \frac{1}{2}(2-y) \right\} \cos \omega t \right\} \right] \quad (17)$$

Skin friction in dust case is

$$Sf_2 = \left( \frac{\partial v_{p1}}{\partial y} \right)_{y=0} = \frac{\tau}{l} \left[ \left\{ \frac{\omega}{2} + 2A\omega - 2B \left( \frac{l}{\tau} + \frac{1}{k} \right) \right\} \sin \omega t + \left\{ -2B\omega + \left( \frac{l}{\tau} + \frac{1}{k} \right) \left( -\frac{1}{2} - 2A \right) \right\} \cos \omega t \right] \quad (18)$$

**Case-2:** When two plates vibrate with same amplitude and frequency, boundary conditions are

$$u(0,t) = u_0 e^{-i\omega t}, \quad u(2y_0,t) = u_0 e^{-i\omega t} \quad [(19)]$$

The dimensionless boundary conditions are

$$[ u(0,t) = e^{-i\omega t}, \quad u(2,t) = e^{-i\omega t} \quad (20)$$

$$\text{Let } u = g(y)e^{-i\omega t} \quad (21)$$

be the solution and proceeding in similar way, we get

$$g''(y) + mg(y) = 0 \quad (22)$$

Where m is given by (13)

Using (20) and (21), we get

$$g(0) = 1 \text{ and } g(2) = 1 \quad (23)$$

The numerical solution of ordinary differential equation (22) subject to boundary conditions (23) using Galerkin technique of finite element analysis is

$$g(y) = 1 + (C+iD)(y^2-2y) \quad (24)$$

The equations (24) and (21) give rise to real part of fluid velocity profile as

$$u_2(y) = \{1 + C\alpha(y^2-2y)\} \cos \omega t + D\alpha(y^2-2y) \sin \omega t \quad (25)$$

Skin friction fluid is given by

$$Sf_3 = \left( \frac{\partial u_2}{\partial y} \right)_{y=0} = -2C\alpha \cos \omega t - 2D\alpha \sin \omega t \quad (26)$$

Equation (6) yields dust velocity

$$v_{p2} = \frac{\tau}{l} \left[ \left\{ D\alpha \left( \frac{l}{\tau} + \frac{1}{k} \right) (y^2-2y) - 2D\alpha - \omega \{ C\alpha(y^2-2y) + 1 \} \right\} \sin \omega t + \left\{ D\alpha\omega(y^2-2y) - 2C\alpha + \left( \frac{l}{\tau} + \frac{1}{k} \right) \{ C\alpha(y^2-2y) + 1 \} \right\} \cos \omega t \right] \quad (27)$$

Skin friction in dust case is

$$Sf_4 = \left( \frac{\partial v_{p2}}{\partial y} \right)_{y=0} = \frac{\tau}{l} \left[ \left\{ 2C\alpha\omega - 2D\alpha \left( \frac{l}{\tau} + \frac{1}{k} \right) \right\} \sin \omega t + \left\{ -2D\alpha\omega - 2C\alpha \left( \frac{l}{\tau} + \frac{1}{k} \right) \right\} \cos \omega t \right] \quad (28)$$

### Results and Discussions:

1. Fluid velocity, dust velocity, related shear stresses at lower plate reduce for higher values of Casson parameter ' $\alpha$ ' and for more than half the distance trend reverses for skin friction, refer figures (5) to (8).

2. Fluid velocity, fluid skin friction and dust shearing stress increase for higher values of permeability parameter ' $k$ ' and trend changes for skin friction in the neighborhood of upper plate as before. There is sudden decrease of velocity for lower values of permeability parameter and gradual reduction is noted for higher value of permeability parameter in case-1, on the whole, permeability parameter subsides dusty flow, refer figures (2) & (4).

3. The concentration ' $l$ ' enhances fluid flow and increases fluid skin friction in case-1 and diminishes the same in case-2.

As concentration increases, dusty velocity decrease attributed to increased number of dust particles and dusty skin friction rises.

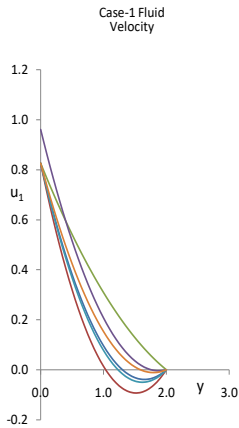


Figure-1

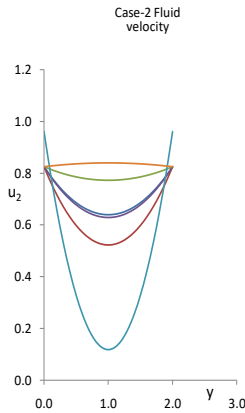


Figure-3

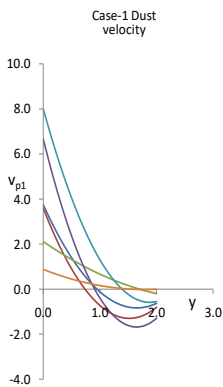


Figure-2

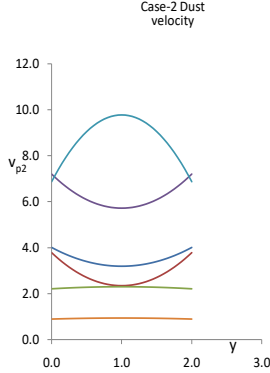


Figure-4

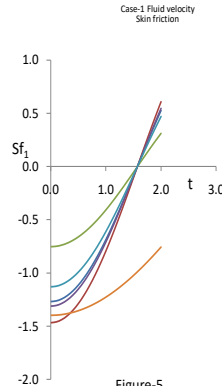


Figure-5

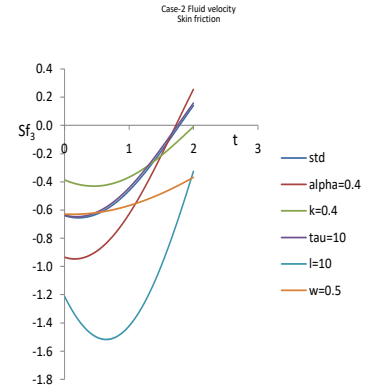


Figure-7

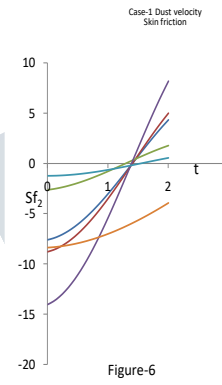


Figure-6

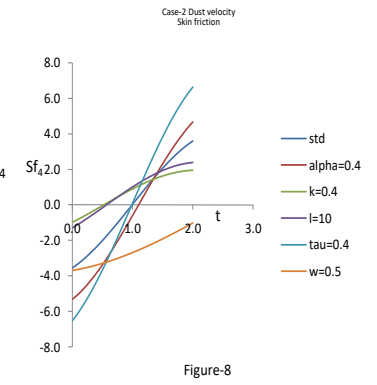


Figure-8

Standard curve data

alpha	k	tau	w	l
0.2	0.2	0.2	1	0.2

4. The relaxation parameter ' $\tau$ ' slightly decreases the fluid velocity and has insignificant effect on fluid skin friction. The time relaxation parameter influences dusty velocity is due to increased time of perturbed state to equilibrium state of dust particles.

5. The frequency parameter ' $\omega$ ' shoots up velocity in case-1 and suppresses the same in case-2 figures (1) & (3). The frequency parameter promotes dust velocity, fluid skin friction and dust skin friction.

**References**

1. J. Majumder and T. Minco (2019), "Advanced Drug Delivery Reviews", Vol.144, pages 57-77.

2. S.A. Hussain, G. Ali, S. Mohammed and S.A. Shaw (2019), "Jour. of Nano Fluids", Vol.8, no.4, pages 714-724.
3. S.A. Hussain, M. Ishaq and S. Mohammed (2018), "Jour. Advanced Physics", Vol.7, no.4, pages 457-464.
4. G. Narender, G. Sharma and K. Goverdhan (2018), "CVR Jour. Sci and Tech.", Vol.15, pages 106-114.
5. Z. Abbas, J. Hasnain and M. Sajid (2019), "Jour. Of Thermophysics", 28, pages 84-102.
6. H. Ali, Attia, K. M. Ewis (2019), "Advances in Mechanical Engineering", SAGE Journals.
7. A. M. Ismail, S. Rahuman and K. S. Kumar (2018), "Int. Jour. of Pure and Applied Mathematics", Vol.119, no.15, pages 1221-1232.
8. R. Sasikala, A.Govinfrajan and R. Gayathri (2018), "Jour. of Physics Conference Series 1000(1):12151.
9. C. K. Selvi and A. N. S. Srinivas, (2018), "Applied Mathematics and Nonlinear Sciences", 3(2), pages 571-582.
10. M. Jalil, S. Asghar and S. Yasmeen (2017), "Mathematical Problems in Engineering", (4): pages 1-5.
11. C. K. Kumar and S. Srinivas, (2017), "Engg. Transactions", 65, 3, pages 461-481.
12. M. A. Imran, S. Sarwar and M. Imran (2016), "Springer Boundary Value problems", Article number 30.
13. A. Khalid, I. Khan, A. Khan and S. Shafi (2015), "International Journal of Science and Technology", Vol.18, Issue 3, pages 309-317.
14. Pramanik, (2014), "Ain Shams Engineering Journal", (5), pages 205-222.
15. S. Singh, P. Kumar, K. N. Rai and N. S. Tomar, (2017), "International Journal of Nonlinear Analysis and Applications", Vol.8, Issue 1, pages 177-186.
16. M. Vidhya, N. Niranjana and A. Govindrajana, (2017), "International Journal of Pure and Applied Mathematics", Vol.114, No.3, pages 445-456.
17. T. G. Prasuna and S. P. Sushma, (2015), "International Journal of Computer and Mathematical Sciences", Vol.4, Issue7.
18. N. Casson (1959), "Rheology of disperse systems" in flow equation for pigment oil suspensions of The printing Ink type, C.C. Mill, Ed. pp 84-102, pergamon press, London, U.K.

**Constants**

$$\begin{aligned}
 a^* &= -1 + \tau k \omega^2, & b &= \omega \{k(1+l) + \tau\}, & a_0 &= k(1 + \omega^2 \tau^2), & a_1 &= a^* - b \omega \tau, \\
 b_1 &= a^* \omega \tau + b, & a_2 &= \frac{a_1}{a_0}, & b_2 &= \frac{b_1}{a_0}, & \alpha_1 &= \frac{1}{a} + 1, \\
 & & b_3 &= 4a a_3 - 10a_2(1 + \alpha), & & & & \\
 a_3 &= a_2^2 + b_2^2, & \alpha_2 &= (8a_3 - 2a_2 \alpha_1)^2 + 400a_1^2 b_2^2, & & & & \\
 & & \alpha_3 &= 5a_3(8a_3 - 2a_2 \alpha_1), & & & & \\
 \alpha_4 &= -20a b_2, & \alpha_5 &= b_3^2 + 100b_2^2, & \alpha_6 &= 5a_3 b_3, & & \\
 & & \alpha_7 &= -150a_3 b_2, & & & & \\
 A &= \frac{\alpha_3}{\alpha_2}, & B &= \frac{\alpha_4}{\alpha_2}, & C &= \frac{\alpha_6}{\alpha_5}, & D &= \frac{\alpha_7}{\alpha_5}
 \end{aligned}$$